

CRC data

Issue no:

Total pages:

First page:

Last page:

File name: B0

Date required:

.TEX

Accuracy of RCC-SD and PT2/CI methods in all-electron and RECP calculations on Pb and Pb²⁺

T A Isaev[†], N S Mosyagin[†], M G Kozlov[†], A V Titov[†], E Eliav[‡] and U Kaldor[‡][†] Petersburg Nuclear Physics Institute, Gatchina, St Petersburg district 188350, Russia[‡] School of Chemistry, Tel Aviv University, Tel Aviv 69978, Israel

E-mail: isaev@dbserv.pnpi.spb.ru

Received 13 July 2000, in final form 6 September 2000

Abstract. Transition energy calculations for low-lying states of Pb and Pb²⁺ by the four-component versions of the Fock-space RCC-SD and PT2/CI methods are reported. Contributions of valence and core electron correlation are studied in all-electron calculations with the Dirac–Coulomb Hamiltonian. The accuracy of our generalized RECP and the RECP of Christiansen and co-workers is tested. The consideration of only one- and two-body amplitudes for valence electrons in the RCC method for Pb is shown not to be sufficient to reproduce valence excitations within 100–300 cm⁻¹. Correcting RCC-SD results by estimated contributions of triple and quadruple excitations yields an accuracy of about 200 cm⁻¹.

1. Introduction

Interest in highly accurate atomic and molecular electronic structure calculations has grown significantly in the last decade, brought about by progress in experimental techniques and in computational methods and capabilities. The Fock-space relativistic coupled-cluster (RCC) method [1–3] has proved to be very economical and reliable within its domain of applicability. It has been applied successfully to calculations of many heavy and super-heavy elements [4, 5] and to several heavy-atom molecules [6, 7].

A combined method of second-order many-body perturbation theory (MBPT2 or PT2) and configuration interaction (CI) [8, 9] was developed recently. In this PT2/CI method, correlation between core and valence electrons is considered by MBPT2, constructing an effective Hamiltonian for valence electrons. The resulting effective Hamiltonian is then used in CI calculations to take into account correlation between valence electrons. The method has been applied to the calculation of excitation spectra and physical properties in heavy atoms [10] and of P, T-odd effects in the BaF and YbF molecules [11].

These methods were shown to be applicable to calculation of atomic transition energies with an accuracy of a few hundred wavenumbers on computers of moderate power, and are therefore promising for accurate studies of heavy-atom molecules. To reduce the computational effort, calculations on such molecules are usually performed with some kind of relativistic effective core potentials (RECPs), and one of the goals of this paper is to estimate the accuracy and reliability of different RECPs before using them in molecular calculations. For low-lying states of the lead atom (with the valence region including two electrons in the open 6p shell and two electrons in the closed 6s shell), relativistic effects are as important as correlation. Pb is

therefore a good test case for methods devised for calculating heavy-atom molecules. Finally, electronic structure calculations on the Pb atom and its ions are also useful for selecting an atomic basis set and determining the number of outer core shells which should be correlated in subsequent calculations of Pb-containing systems to obtain the desired accuracy.

2. Methods

A detailed description of the RCC and PT2/CI methods may be found in [1, 2, 12] and in [8, 9, 13], respectively. The theory of generalized RECP (GRECP) and other shape-consistent RECPs (with orbitals smoothed in the atomic core region) is presented in [14]. Only a brief review of these methods is given below.

2.1. Relativistic coupled-cluster method

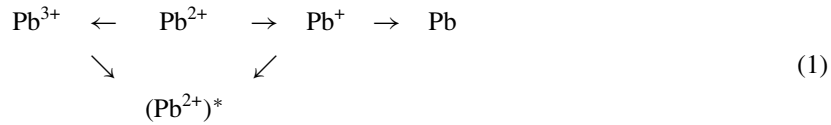
The sectors of the Fock space with m holes and n particles with respect to some reference closed-shell state are denoted by (m, n) . The wavefunction in the Fock-space coupled-cluster (CC) method is first calculated in the $(0, 0)$ sector. It is presented in the form

$$|\Psi\rangle = e^T |\Phi\rangle$$

where e^T is the exponential wave operator and $|\Phi\rangle$ is a zero-order function of some reference closed-shell state. Correlation effects for this state are taken into account by the operator T , which is usually truncated at some excitation level (thus, only one- and two-body amplitudes are included in the RCC method with single and double excitations, or RCC-SD). At the next step, the number of electrons in the system is increased or decreased by one electron (sectors $(0, 1)$ and $(1, 0)$, respectively) and the system is ‘recorrelated’

$$|\Psi_j\rangle = e^T \sum_i C_{ij} b_i^+ |\Phi\rangle$$

where b_i^+ is the creation operator for a hole or particle in the i th valence one-electron state. Because the amplitudes calculated in the $(0, 0)$ sector are not varied at this step, only a small fraction of the cluster amplitudes is now calculated in the T operator. One more electron is then added to or removed from the system, and the cluster amplitudes for low-lying states are obtained for the systems of $(N+2)$, N and $(N-2)$ electrons (sectors $(0, 2)$, $(1, 1)$ and $(2, 0)$). Spherical symmetry and the jj -coupling scheme are used, allowing analytic integration over angular and spin variables, with considerable computational savings. The Fock-space scheme used in this paper is



with electrons added in the $6p_{1/2}$ and $6p_{3/2}$ spinors and removed from the $6s_{1/2}$ spinor.

2.2. Combined PT2/CI method

The Hilbert space, where the many-electron equation

$$H|\Psi\rangle = E|\Psi\rangle \tag{2}$$

is defined, is partitioned into two subspaces, P and Q . The corresponding projection operators P and Q satisfy the relation $P + Q = \mathbf{1}$. The operator P is defined as the projector on those states of the atom in which the one-electron core states are always occupied. One may write

$$\begin{aligned} H &= PHP + PHQ + QHP + QHQ \\ |\Psi\rangle &= P|\Psi\rangle + Q|\Psi\rangle \equiv |\phi\rangle + |\chi\rangle. \end{aligned}$$

In the conventional CI calculation (in the model space defined by the projector P) the equation solved is

$$(PHP)|\phi_{\text{CI}}\rangle = E_{\text{CI}}|\phi_{\text{CI}}\rangle.$$

The solution of this equation differs from that of equation (2), because the Q subspace is not taken into account. Accounting for Q leads to the CI equation

$$(PHP + \Sigma(E))|\phi\rangle = E|\phi\rangle \quad (3)$$

where

$$\Sigma(E) = (PHQ) \frac{1}{E - QHQ} (QHP).$$

The operator $\Sigma(E)$ with the proper orbital choice may be written as

$$\Sigma(E) = P(V - V^{N_{PT}})Q \frac{1}{E - QHQ} Q(V - V^{N_{PT}})P \quad (4)$$

where V is the two-electron Coulomb (electrostatic) interaction and $V^{N_{PT}}$ is the Hartree–Fock potential of N_{PT} electrons. The value of N_{PT} must satisfy the condition $N_c \leq N_{PT} \leq N$, where N_c is the number of core electrons and N is the total number of electrons in the system. The $\Sigma(E)$ operator is calculated by standard diagrammatic techniques within the framework of the Brillouin–Wigner PT2 with some approximation for E (the E values used here are described in section 4.1 below), and equation (3) is then solved by the CI method. It should be noted that the basis sets used for calculating the $\Sigma(E)$ operator and for solving equation (3) need not be identical.

2.3. Shape-consistent RECPs and GRECP

The Dirac–Coulomb (DC) or Dirac–Coulomb–Breit (DCB) Hamiltonian, H^{rel} , is replaced in RECP calculations by an effective Hamiltonian

$$H^{\text{eff}} = H^{\text{non-rel}} + U^{\text{eff}} \quad (5)$$

where $H^{\text{non-rel}}$ is the Schrödinger Hamiltonian written only for some (pseudo)valence electrons and U^{eff} is an RECP operator simulating interactions of the (pseudo)valence electrons with the electrons excluded from the RECP calculations. Contrary to the four-component wavefunction used in DC(B) calculations, the pseudo-wavefunction in the RECP case can be two- or one-component.

In the shape-consistent RECP calculations, the radial oscillations of the valence spinors are smoothed in the core region. The components of the effective potential, $U_{nlj}(r)$, are derived by inversion of the non-relativistic-type Hartree–Fock equation in the jj -coupling scheme for a ‘pseudo-atom’ with the core electrons removed,

$$\begin{aligned} U_{nlj}(r) = \tilde{\varphi}_{nlj}^{-1}(r) \left[\left(\frac{1}{2} \frac{d^2}{dr^2} + \frac{1}{r} \frac{d}{dr} - \frac{l(l+1)}{2r^2} + \frac{Z^*}{r} - \tilde{J}(r) + \tilde{K}(r) + \varepsilon_{nlj} \right) \tilde{\varphi}_{nlj}(r) \right. \\ \left. + \sum_{n' \neq n} \varepsilon_{n'nlj} \tilde{\varphi}_{n'lj}(r) \right] \quad (6) \end{aligned}$$

where $Z^* = Z - N_c$ is the effective (nuclear and core) charge, \tilde{J} and \tilde{K} are the Coulomb and exchange operators calculated with the pseudospinors $\tilde{\varphi}_{nlj}$, ε_{nlj} are the one-electron energies of the corresponding spinors, and $\varepsilon_{n'lj}$ are the off-diagonal Lagrange multipliers.

The principal features distinguishing the generalized RECP version used here from conventional semilocal RECP versions are: (a) the GRECP generation scheme involves valence (V) and outer core (OC) pseudospinors with the same angular (l) and total (j) momenta; (b) the GRECP operator includes non-local terms [15] in addition to the standard radially local operator. The innermost outer core pseudospinors have nodeless radial functions, whereas the valence pseudospinors have nodal radial parts. The problem of dividing by zero, which arises for pseudospinors with nodes, is overcome by interpolating the corresponding potential in the vicinity of the node. The expression for the GRECP operator is

$$\begin{aligned} U^{\text{GRECP}} = & U_{n_v L J}(r) + \sum_{l=0}^L \sum_{j=|l-1/2|}^{l+1/2} [U_{n_v l j}(r) - U_{n_v L J}(r)] P_{lj} \\ & + \sum_{n_c}^L \sum_{l=0}^L \sum_{j=|l-1/2|}^{l+1/2} \left\{ [U_{n_c l j}(r) - U_{n_v l j}(r)] \tilde{P}_{n_c l j} + \tilde{P}_{n_c l j} [U_{n_c l j}(r) - U_{n_v l j}(r)] \right\} \\ & - \sum_{n_c, n'_c}^L \sum_{l=0}^L \sum_{j=|l-1/2|}^{l+1/2} \tilde{P}_{n_c l j} \left[\frac{U_{n_c l j}(r) + U_{n'_c l j}(r)}{2} - U_{n_v l j}(r) \right] \tilde{P}_{n'_c l j} \end{aligned} \quad (7)$$

where

$$\begin{aligned} P_{lj} &= \sum_{m_j=-j}^j |l j m_j\rangle \langle l j m_j| \\ \tilde{P}_{n_c l j} &= \sum_{m_j=-j}^j |\widetilde{n_c l j m_j}\rangle \langle \widetilde{n_c l j m_j}| \end{aligned}$$

$|l j m_j\rangle \langle l j m_j|$ is the projector on the two-component spin-angular function $\chi_{l j m_j}$, $|\widetilde{n_c l j m_j}\rangle \langle \widetilde{n_c l j m_j}|$ is the projector on the outer core pseudospinor $\tilde{\varphi}_{n_c l j} \chi_{l j m_j}$, L is larger by one than the highest orbital angular momentum of the inner core (removed) spinors, and $J = L + \frac{1}{2}$. The first line in equation (7) presents the standard radially local RECP operator U^{RECP} . In equation (5) and below U^{eff} denotes either U^{RECP} or U^{GRECP} , depending on the RECP version used. As pointed out earlier [14, 16], the form (7) of the GRECP operator is optimal for the calculation of states in which the occupation numbers of the outer core shells are approximately the same as in the state used for the GRECP generation (i.e. the leading configurations have no excitations from the outer core shells).

3. Generation and optimization of basis set

The basis set for all-electron and RECP calculations of Pb was largely generated by the scheme suggested in [17]. Ideas taken from ANO [19] and correlation-consistent [20] basis set generation schemes were also employed. Basis spinors were obtained from SCF calculations (Dirac–Fock or Hartree–Fock with RECP) for different configurations of the neutral Pb atom and its positive ions. We used the HFD code [21] for all-electron four-component calculations and its modified version, HFJ [22], for two-component calculations with RECPs. SCF calculations were first performed for the ground $6s^2$ state of the Pb^{2+} ion, yielding the $1s_{1/2}, \dots, 6s_{1/2}$ spinors. The $6p_{1/2,3/2}$ spinors were then obtained as solutions of

the SCF equation for the state of Pb averaged over the non-relativistic $[6s^2]6p^2$ configuration. The notation $[6s^2]6p^2$ indicates that all orbitals up to and including the orbital in square brackets (6s in this case) are frozen after the SCF calculation of the relevant species (Pb²⁺ here).

The next stage consisted of a number of SCF calculations for neutral and a sequence of ionized states of Pb with the configurations $[6s^26p^1]7s^1$, $[6s^n]7s^1$ ($n = 1, 2$), $[5d^n]7s^1$ ($n = 1, 2, \dots, 10$), etc. The 7s spinors generated are thus localized in different spatial regions. A sequence of basis sets is formed by adding one of these spinors to the initial basis set. The added spinor is orthogonalized to the other spinors of the same symmetry in the basis, and the Fock operator constructed for the $6s^2$ state is diagonalized in the basis obtained. The Pb atom low-lying states of interest are then calculated by some correlation method (CI, PT2/CI or RCC) for each basis set, and the basis for which an energy functional $\mathcal{F}(\Delta E_1, \dots, \Delta E_M)$ is the largest is selected. $\Delta E_i \geq 0$ is the lowering of the energy E_i of the i th state with respect to the initial basis set, and M is the number of states considered. The same procedure is then repeated for the pair of spinors $7p_{1/2}$ and $7p_{3/2}$, with the initial basis set taken from the previous step. New functions are added in a similar fashion, until the functional \mathcal{F} becomes smaller than some threshold T . In [17] we used the functional

$$\mathcal{F}(\Delta E_1, \dots, \Delta E_M) = \max_{i>j}^M |\Delta E_i - \Delta E_j| \quad (8)$$

here the average energy lowering for the states selected is used as the energy functional,

$$\mathcal{F}(\Delta E_1, \dots, \Delta E_M) = \frac{1}{M} \sum_i^M \Delta E_i. \quad (9)$$

The process of basis set generation is terminated when the energy functional goes below the threshold $T = 50 \text{ cm}^{-1}$. In a more sophisticated treatment, the two functionals may be applied consecutively in the basis set generation, with functional (9) used at the first stage. Such a scheme may be more appropriate for generating basis sets to be used in subsequent molecular calculations; an implementation is now in progress. Theoretical justification for the combined selection scheme may be found in [23].

The resulting basis set, consisting of three s-spinors, five pairs of p-spinors, three pairs of d-spinors and two pairs of f-spinors (denoted by [3, 5, 3, 2]), was used for valence CI calculations. Different basis sets may be used to take account of the V–V and OC–V correlations in the

Table 1. Errors in all-electron transition energies of the Pb atom obtained by the RCC-SD and PT2/CI methods for states with $6s^26p^2$ configuration. All values are in cm^{-1} .

Term	Experimental transition energies	Errors ^a in transition energies							
		RCC-SD				CI		PT2/CI	
		Number of correlated electrons							
		4	14	22	36	4	14	22	36
³ P ₀	0	0	0	0	0	0	0	0	0
³ P ₁	7 819	–1161	–630	–450	–414	–807	–535	–393	–365
³ P ₂	10 650	–1229	–539	–364	–320	–752	–428	–294	–282
¹ D ₂	21 457	–2263	–963	–618	–530	–1707	–849	–573	–402
¹ S ₀	29 466	–1362	–70	199	291	–1553	–270	–33	90
Max. error		2263	963	817	821	1707	849	573	492
Average error		945	497	417	411	843	392	301	270

^a Errors were taken as differences between calculated values and experimental data (in column 2).

PT2/CI calculations and, therefore, an optimal ‘double’ basis set for the PT2/CI calculations was generated: the CI part of the basis set was kept unchanged, and the PT2 subset was obtained by adding the spinors to the CI part by the procedure described above. The optimization was performed for 36 correlated electrons (down to the 4f shell) and a ‘double’ PT2/CI basis set, [7, 6, 6, 4, 4]/[3, 5, 3, 2], was generated.

We estimate the contributions of higher harmonics (functions with $l > 4$) in the energy functional to be at most 100 cm^{-1} †. The results of calculations with the basis sets generated are presented in table 1 and discussed below. Although substantially more extensive basis sets can be used in atomic calculations, different optimization procedures are studied in our papers in order to minimize the atomic basis set size which provides a given (high) accuracy in subsequent molecular calculations.

4. Results and discussion

Transition energies for the five lowest-lying states of the Pb atom were calculated using the PT2/CI and RCC-SD methods, employing both the all-electron Dirac–Coulomb Hamiltonian and the non-relativistic-type RECP Hamiltonian. The accuracy of our generalized RECP [16] and the RECP of Christiansen and co-workers [24] (denoted below as ‘ChRECP’ for brevity) was tested in calculations on neutral Pb atom and the Pb^{2+} ion. For both RECPs, the 22 outermost valence and outer core electrons are included explicitly in the Pb calculations (20 electrons for Pb^{2+}). Below we refer to the 6s and 6p shells as valence and to the 5d, 5p and lower shells as core. A point nucleus model was employed in all calculations. The effect of a finite nucleus model is not expected to be large for transition energies of the Pb atom, because the 6s electrons (which have a non-vanishing density on the Pb nucleus) are not excited in the leading configurations of all the states considered (see our results for the Hg atom [17]). In all tables the maximum error is $\max_{i>j}^M |\delta E_i - \delta E_j|$, the average error is $2 \sum_{i>j}^M |\delta E_i - \delta E_j| / [M(M-1)]$ and $\delta E_i = E_i^{\text{RECP}} - E_i^{\text{DC}}$.

4.1. Contribution from correlation with core shells

The calculated transition energies are presented in table 1. The basis sets [3, 5, 3, 2], [7, 6, 6, 4, 4]/[3, 5, 3, 2] and [7, 6, 6, 4, 4] were used in the four-electron CI (4e–CI), PT2/CI and RCC-SD calculations, respectively. The basis set for RCC-SD is identical with the PT2 part of the PT2/CI basis. The average 4e–CI energy of the five lowest-lying Pb levels was used as the E value in equation (4). Varying E by 0.1 Hartree changes the final transition energies by less than 50 cm^{-1} .

The biggest error in the 4e–CI excitation energies with respect to the experimental data, 1707 cm^{-1} , goes down to 492 cm^{-1} when 36 electrons are correlated. As expected, the biggest OC–V contribution to the transition energies comes from correlation with the 5d shell (see the 14e-PT2/CI and RCC-SD results in table 1). The corresponding contribution to transition energies is up to 1300 cm^{-1} . A rather large contribution from correlating the 4f shell (up to 170 cm^{-1}) is due to the fact that this shell is energetically close to the outer core shells. Despite the relatively small average radius, the orbital energies of 4f spinors are very close to those of 5s spinors.

We performed a detailed analysis of the correlations with the 4f shell on the basis of RCC-SD calculations. It shows that angular OC–V correlation, described by excitations of occupied to virtual orbitals with similar radial distribution but different angular momentum of the type

† See [18] for details of the optimization.

(4f, 6p) \rightarrow (g, d) and (4f, 6s) \rightarrow (g, p), gives the main contribution of the 4f shell to transition energies studied. Contribution from the former type of excitations is at the 50–150 cm^{-1} level for different terms and has the opposite sign to the contribution from the excitations of the latter type, which is at the level 20–50 cm^{-1} (see [18] for details). In the case of 5s and 5p shells angular correlation of this kind is suppressed; for example, (5p, 6p) \rightarrow (5d, d) is forbidden because the 5d shell is occupied.

4.2. Accuracy of RECPs

Errors in calculated transition energies caused by the ChRECP and GRECP approximations are studied by comparing the RECP and all-electron Dirac–Coulomb calculations. The correlation basis set [3, 5, 3, 2] described in section 3 is used for the 4e–CI and 4e–RCC calculations. Preliminary RECP calculations have shown that it is preferable to optimize the basis sets independently for DC, GRECP and ChRECP calculations accounting for OC-V correlation, in order to attain satisfactory convergence of the total energies. To minimize the computational effort at the basis set generation stage, a simplified generation scheme was used which, nevertheless, demonstrated excellent agreement for the DC/RCC excitation energies compared with the results presented in table 1 (with the basis sets described in section 3). For each Hamiltonian (GRECP, ChRECP and all-electron DC), a scheme close to that described in section 3 is used: first, a few spinors in each symmetry are obtained from Hartree–Fock calculations of some atomic or ionic states and are selected with the help of the functional (9). The next function is then derived by multiplying the radial part (in all-electron calculations the radial part of the large component) of the last selected function of the same symmetry by the radial variable r (see [9]). The corresponding small components for four-component functions are formed using the ‘kinetic balance’ condition. Functions of the same symmetry are orthogonalized and correlation calculations are performed. The basis set is extended until the energy functional is not more than 50 cm^{-1} (see section 3). This procedure yielded a [15, 14, 12, 8] correlation basis set for the 14e, 22e–RCC and 14e, 22e–PT2/CI calculations of Pb. The same procedure was applied to Pb^{2+} and gave the basis sets [6, 6, 8, 5, 4] for 2e–CI and [15, 14, 12, 8] for 12e, 20e–RCC.

The results of the RECP/RCC and RECP/PT2/CI calculations for the $6p^2$ states of Pb are presented in table 2 (see also table 1 in [18]). The accuracy of the GRECP approximation for these states is on average only about 1.5 times better than that of ChRECP. Similar calculations for the $6s^2 \rightarrow 6s6p$ transitions in Pb^{2+} (table 3) show a different picture, with GRECP giving an average accuracy about eight times higher and a maximum error more than 10 times lower compared with ChRECP values. It should be noted that ChRECP errors in this case have different signs for valence CI and 12e, 20e–RCC-SD. Thus, the two RECPs are satisfactory for describing the excitation spectrum of Pb, whereas GRECP is much better for Pb^{2+} excitations, indicating that GRECP treats the 6s shell of Pb more accurately than ChRECP.

It has been shown earlier [14, 16, 22] that the GRECP version applied here gives no great improvement for transition energies between terms with the same electron configuration as compared with the conventional (‘ionic’) RECP versions treating the same number of electrons explicitly. This may be understood by considering the term-splitting energies within the framework of the Rayleigh–Schrödinger perturbation theory (PT) for the corresponding spin-adapted (and spatial-symmetry-adapted) wavefunctions (SAFs). Let us construct zero-order approximations for the SAFs from the occupied spin-orbitals of a one-configurational generator state averaged over the terms, so the SAFs describing the terms of interest are eigenfunctions of the same unperturbed spin-independent Hartree–Fock Hamiltonian $H^{(0)}$ (which is, obviously, a Hartree–Fock operator for the generator state). The energies of the terms are degenerate

Table 2. Errors^a of RECP calculations in reproducing the corresponding all-electron transition energies (in table 1) of low-lying states of Pb. Experimental energies appear in table 1. All values are in cm^{-1} .

Term ^b	RCC-SD						PT2/CI					
	GRECP ^c			ChRECP ^d			GRECP ^c			ChRECP ^d		
	Number of correlated electrons											
	4	14	22	4	14	22	4	14	22	4	14	22
³ P ₀	0	0	0	0	0	0	0	0	0	0	0	0
³ P ₁	12	67	57	17	74	79	26	56	69	31	63	58
³ P ₂	13	57	52	35	74	85	36	62	77	38	67	66
¹ D ₂	24	84	86	75	120	169	46	89	120	76	82	81
¹ S ₀	48	103	107	76	128	152	57	90	127	77	149	161
Max. error	48	103	107	76	128	169	57	90	127	77	149	161
Av. error	22	47	50	44	60	82	27	43	65	40	69	63

^a In this table, errors were calculated as differences between transition energies from RECP and corresponding all-electron calculations (in table 1). The point nucleus model is employed.

^b The leading configuration is $6s^26p^2$.

^c GRECP from [16, 22].

^d RECP of Christiansen's group [24].

Table 3. Errors^a of RECP calculations in reproducing the corresponding all-electron transition energies (in columns 4–6) of low-lying states of Pb²⁺. All values are in cm^{-1} .

Conf. (Term)	Exper. trans. energ.	All-electron			GRECP ^b			ChRECP ^c		
		Number of correlated electrons								
		2	12	20	2	12	20	2	12	20
$6s^2(^1S_0)$	0	0	0	0	0	0	0	0	0	0
$6s^16p^1(^3P_0)$	60 397	55 130	61 657	61 661	-40	-187	-192	-279	1247	1292
$6s^16p^1(^3P_1)$	64 391	59 706	65 787	65 833	-43	-177	-173	-295	1312	1318
$6s^16p^1(^3P_2)$	78 984	73 857	79 868	80 130	-45	-105	-122	-358	1439	1504
$6s^16p^1(^1P_1)$	95 340	95 474	97 966	98 244	-131	-52	-27	-431	2049	2035
Max. error					131	187	192	431	2049	2035
Av. error					53	103	106	187	858	856

^a In this table, errors were calculated as differences between transition energies from the RECP and corresponding all-electron calculations (in columns 4–6) by RCC-SD (12 and 20 electrons) or CI (two electrons). The point nucleus model is employed.

^b GRECP from [16, 22].

^c RECP of Christiansen's group [24].

in zero order. The degeneracy is removed in first order, in which the perturbation on the spin-orbit and two-electron interactions usually provide good approximations to the exact term-splitting energies. The spin-averaged one-electron part of the Hamiltonian, including, obviously, the non-local GRECP terms in the case of the GRECP Hamiltonian, gives no contribution in first order; its contribution will appear only in the denominators of higher PT orders. Although the spin-orbit part of RECPs contributes to the term-splitting energies in first-order PT, the difference between GRECP and ChRECP contributions is minor because of the relative smallness of the non-local spin-orbit GRECP terms. In excitations which change the electron configuration, the PT contribution from the non-local spin-averaged GRECP terms appears already in zero order. More details may be found in the section 'Theory' of [14]. It is worth mentioning that errors given by conventional RECPs for term-splitting energies are

usually smaller than for excitation energies which change the occupation numbers of valence shells, as may be seen by comparing tables 2 and 3.

The SCF results [18] show that the accuracy of the ChRECP corresponds closely to that of our ionic RECP version [22]. In principle, the GRECP technique allows one to reduce substantially the ‘correlation-stage’ RECP errors (see [14]). This is, however, of limited interest, because the GRECP approximation is not the main source of errors in calculations of Pb-containing molecules. A more serious source of error is discussed in the next subsection.

4.3. Contribution from three- and four-particle correlations

Table 1 shows that single- and double-excitation cluster amplitudes are not sufficient to give the Pb transition energies at an accuracy level of $\sim 200 \text{ cm}^{-1}$. This is also indicated by comparing the 4e-RCC-SD with 4e-CI total energies (table 4). Since the latter is close to full 4e-CI (some of the less important quadruple excitations are omitted, and the estimated deviation from full 4e-CI is about 50 cm^{-1} for transition energies and 100 cm^{-1} for total energies), the differences are ascribed to neglecting the three- and four-electron excitations in the former. These terms are significant, except for the 1D_2 level, for which the total energies are almost equal. Analysing the correlation structure for four-valence electrons in the 1D_2 and 1S_0 terms, the different behaviour appearing already for the (s, p) basis set (table 4) shows that some four-electron correlation terms not allowed in the 1D_2 state because of symmetry are significant for the 1S_0 state and are not described by the RCC-SD approximation used here. Let us consider virtual excitations for the component of the 1D_2 level with maximum projection on the z-axis, $J_z = 2$, which has the leading configuration $6s_{1/2}^2 6p_{3/2,+1/2} 6p_{3/2,+3/2}$. No non-trivial triple- and quadruple excitations of the type ($6s^2 6p^2 \rightarrow 6p^4$) are allowed from this configuration, since J_z must be conserved. These excitations describe polarization of the valence electrons and, in particular, admixture of their tetrahedral configuration, which

Table 4. Contributions from triple- and quadruple-excitation amplitudes to Pb total state energies and errors for the VCIC-corrected values of transition energies. Experimental energies appear in table 1. All values are in cm^{-1} .

Term (leading configuration)	Basis set			Errors in transition energies ^b		
	[3, 5] Δ^a	[3, 5, 3] Δ^a	[3, 5, 3, 2] Δ^a	Number of correlated electrons		
	4	4	4	14	22	36
$^3P_0 (6s_{1/2}^2 6p_{1/2}^2)$	-334	-690	-586	0	0	0
$^3P_1 (6s_{1/2}^2 6p_{1/2}^1 6p_{3/2}^1)$	-120	-389	-232	-276	-96	-60
$^3P_2 (6s_{1/2}^2 6p_{1/2}^1 6p_{3/2}^1)$	-104	-242	-109	-62	113	157
$^1D_2 (6s_{1/2}^2 6p_{3/2}^2)$	-11	47	-30	-407	-62	26
$^1S_0 (6s_{1/2}^2 6p_{3/2}^2)$	-412	-680	-777	-261	8	100
Max. error	412	737	777	407	209	217
Av. error	196 ^c	410 ^c	347 ^c	206	88	106

^a $\Delta_i = E_i^{\text{CI}} - E_i^{\text{RCC}}$.

^b Errors were taken as differences between calculated values (by RCC-SD + VCIC) and experimental data (in column 2 of table 1).

^c $\Delta_{\text{av}} = \frac{1}{5} \sum_{i=1}^5 |E_i^{\text{CI}} - E_i^{\text{RCC}}|$.

minimizes the interelectronic repulsion energy for four electrons. The opposite is true for the 1S_0 state, for which these triple and quadruple excitations provide some of the most important correlation contributions.

The non-negligible differences between 4e-RCC-SD and 4e-CI values come from omitting three- and four-body cluster amplitudes in RCC-SD. The relevant wavefunction diagrams include connected three- and four-body terms, which first appear in second- and third-order PT, respectively. The energy difference between the 1D_2 and 1S_0 states stays almost the same when the number of correlated electrons in the RCC-SD method is increased from four to 36. The effect of triple- and quadruple-cluster amplitudes for the valence electrons (from the physical point of view these amplitudes also correct the single and double amplitudes obtained in the subduced sectors) can be estimated from the valence CI corrections (VCIC), the differences ($E_i^{4e-CI} - E_i^{4e-RCC}$), which are then added to the other total N e-RCC-SD energies ($N = 14, 22, 36$). The assumption involved is that the effect of the triple- and quadruple-cluster amplitudes for valence electrons estimated from 4e-RCC-SDTQ calculations (which are equivalent to four-electron full CI) will not change much when more electrons are treated and OC-V and OC-OC correlation is included. It should be noted that those three- and four-body terms, not taken into account by RCC-SD in the valence region, cannot be satisfactorily included by extending the model space within the Fock-space RCC-SD method. The RCC-SD results corrected for three- and four-body effects by VCIC are shown in table 4. Agreement with experiment is improved greatly over uncorrected RCC-SD values, reaching the desired level of $\sim 200 \text{ cm}^{-1}$ for 22 and 36 correlated electrons.

5. Concluding remarks

We suggest that inclusion of estimated triple and quadruple valence excitation effects can significantly increase the accuracy of the RCC results. Breit effects should also be included at this level of accuracy. The contribution of the Breit term to the spin-orbit splitting of the Tl ground state (i.e. the $6p_{1/2} \rightarrow 6p_{3/2}$ excitation) has been calculated at -90 cm^{-1} [25]. Assuming a similar relative effect in the case of Pb, rough estimates would give contributions of about -100 cm^{-1} to the first two transitions and about -200 cm^{-1} to the third and fourth transitions.

In accurate calculations of Pb-containing molecules it would be preferable to include correlation with the 4f, 5s and 5p shells within the framework of the ‘correlated’ RECP versions and not explicitly, thus reducing the computational effort. In this case the generation of the ‘correlated’ GRECP for Pb is of particular importance, because it allows one to minimize the errors of the RECP approximation which, otherwise, can be comparable with the correlation errors.

We should note that the current version of the atomic RCC-SD codes is substantially faster than the PT2/CI codes for equivalent calculations. The high speed of atomic RCC-SD calculations can be used efficiently in the generation of optimal (compact) basis sets for correlation structure calculations of molecules containing Pb and other heavy atoms.

Acknowledgments

This work was supported by the INTAS grant no 96-1266. TI, NM and AT were also sponsored by the RFBR (grant no 99-03-33249) and DFG/RFBR (grant no 96-03-00069). MK is grateful to RFBR for the financial support by grant no 98-02-17663. Work at TAU was supported by the Israel Science Foundation and by the US-Israel Binational Science Foundation. The authors

are grateful to P Christiansen for sending us a recent (unpublished) version of the 22-electron RECP.

References

- [1] Kaldor U and Eliav E 1998 *Adv. Quantum Chem.* **31** 313
- [2] Ilyabaev E and Kaldor U 1992 *Phys. Rev. A* **47** 137
- [3] Shukla A, Das B P and Mukherjee D 1994 *Phys. Rev. A* **50** 2096
- [4] Eliav E and Kaldor U 1995 *Phys. Rev. A* **52** 291
- [5] Eliav E, Kaldor U and Ishikawa Y 1996 *Phys. Rev. A* **53** 3050
- [6] Eliav E, Kaldor U and Hess B A 1998 *J. Chem. Phys.* **108** 3409
- [7] Pernpointner M, Schwerdtfeger P and Hess B A 1998 *J. Chem. Phys.* **108** 6739
- [8] Dzuba V A, Flambaum V V and Kozlov M G 1996 *Phys. Rev. A* **54** 3948
- [9] Kozlov M G and Porsev S G 1997 *Sov. Phys.-JETP* **84** 461
- [10] Porsev S G, Rakhlina Yu G and Kozlov M G 1999 *J. Phys. B: At. Mol. Opt. Phys.* **32** 1113
- [11] Kozlov M G, Titov A V, Mosyagin N S and Souchko P V 1997 *Phys. Rev. A* **56** R3326
Titov A V, Mosyagin N S and Ezhov V F 1996 *Phys. Rev. Lett.* **77** 5346
- [12] Kaldor U 1995 *Few-Body Syst. Suppl.* **8** 68
- [13] Dzuba V A, Kozlov M G, Porsev S G and Flambaum V V 1998 *ZhETF* **114** 1636
- [14] Titov A V and Mosyagin N S 1999 *Int. J. Quant. Chem.* **71** 459
- [15] Titov A V, Mitrushenkov A O and Tupitsyn I I 1991 *Chem. Phys. Lett.* **185** 330
- [16] Mosyagin N S, Titov A V and Latajka Z 1997 *Int. J. Quant. Chem.* **63** 1107
- [17] Mosyagin N S, Eliav E, Titov A V and Kaldor U 2000 *J. Phys. B: At. Mol. Opt. Phys.* **33** 667
- [18] <http://www.qchem.pnpi.spb.ru/publication/pb-ci-pt>
- [19] Almlöf J and Taylor P R 1987 *J. Chem. Phys.* **86** 4070
- [20] Dunning T H, Jr 1989 *J. Chem. Phys.* **90** 1007
- [21] Bratzev F V, Deyneka G B, Tupitsyn I I 1977 *Bull. Acad. Sci.* **41** 173
- [22] Tupitsyn I I, Mosyagin N S and Titov A V 1995 *J. Chem. Phys.* **103** 6548
- [23] Titov A V 1993 *Int. J. Quant. Chem.* **45** 71
- [24] Wildman S A, DiLabio G A and Christiansen P A 1997 *J. Chem. Phys.* **107** 9975
Christiansen P A 1999 Private communication
- [25] Landau A, Eliav E and Kaldor U 1999 *Poster presented at the European Research Conf. Relativistic Quantum Chemistry - Progress and Prospects (Acquafredda di Maratea, Italy, 10–5 April 1999)*